

Deconfinement and Thermodynamics in 5D Holographic Models of QCD

U. Gürsoy,

*Institute for Theoretical Physics, Utrecht University; Leuvenlaan 4, 3584 CE
Utrecht, The Netherlands.*

ABSTRACT: We review 5D holographic approaches to finite temperature QCD. Thermodynamic properties of the “hard-wall” and the “soft-wall” models are derived. Various non-realistic features in these models are cured by the set-up of improved holographic QCD, that we review here.

KEYWORDS: QCD; Holography; Thermodynamics.

Contents

1. Introduction	1
2. Thermodynamics of the AdS/QCD Models	2
2.1 Hard-wall model	2
2.2 Thermodynamics of the Hard-Wall	3
2.3 Soft-wall model	5
2.4 Thermodynamics of the Soft-Wall	7
3. Non-critical holographic QCD	7
3.1 Dynamical Models	7
3.2 Improved holographic QCD	8
4. Thermodynamics of Improved Holographic QCD	11
5. Discussion and Outlook	15

1. Introduction

Recent experimental results indicate that the quark-gluon plasma produced in the heavy-ion collisions stays strongly coupled at temperatures above deconfinement [1]. Therefore understanding the nature of QCD matter at high temperature and density requires non-perturbative techniques. Lattice QCD, being an intrinsically Euclidean formulation is not well-suited for calculating certain important dynamical observables such as transport coefficients or any sort of real-time correlation functions.

For this reason holographic techniques based on the AdS/CFT correspondence [2], have recently attracted much attention in study of such dynamical phenomena. For example the shear viscosity [3], jet quenching parameter [4] and the drag force [5] has been calculated with better success than corresponding perturbative findings.

One approach for constructing gravitational backgrounds dual to QCD-like theories, is to search for deformations of ten dimensional $AdS_5 \times S^5$ background that breaks supersymmetry and conformality. Such models [6] enjoyed success in reproducing certain IR phenomena but they also bear some non-realistic features such as presence of KK modes arising from the extra dimensions. Another, more phenomenological approach [7], instead of attempting at deriving QCD from fundamentals of 10D critical string theory, aims at deriving a 5D gravitational background from the

basic requirements of QCD. This idea goes under the name of AdS/QCD[8] and also achieved partial success, especially in the meson sector.

Generally, finite temperature in the holographic approach is introduced by compactifying the Euclidean time direction with period $1/T$. One such obvious solution is the thermal graviton gas. Other more non-trivial solutions involve black-holes. The black-hole solutions correspond to the deconfined phase of the corresponding gauge theory [9], hence encode physics above the deconfinement transition. The purpose of this paper is to review the thermodynamics in the aforementioned 5D models.

In the next section, we review the thermodynamic properties of the AdS/QCD models based on the hard-wall (HW) and the soft-wall (SW) geometries. By extending the analysis of [10], we compute quantities such as the energy, entropy and speed of sound as functions of T and compare them with the expectations from the lattice. Unlike the HW, the SW model shows good agreement with the lattice data. However, being a non-dynamical model the black-holes in this geometry do not obey the laws of BH thermodynamics. From a practical point of view this fact renders computation of certain quantities like the bulk viscosity ill-defined. Moreover, it does not give insight in the nature of the deconfinement transition.

In section 3, we study a dynamical model based on dilaton-gravity [11, 12] which is close in many respects to real QCD. This model is based on general expectation of stringy holographic QCD whose thermodynamic properties were derived in [13]. We show that this background solves most of the problems in the AdS/QCD models at once, sheds light on the role of the gluon condensate in the phase transition and yields very good agreement with the lattice data. In the final section, we summarize the results, and discuss further directions.

2. Thermodynamics of the AdS/QCD Models

2.1 Hard-wall model

The simplest 5D holographic model for QCD is introduced in [8]. The idea is based on the fact that QCD behaves nearly scale invariant for a wide range of energies ranging from far UV down to medium energy scales. Thus the authors of [8] proposed a geometrical set-up based on the 5D AdS space with a cut-off in the deep-interior of the holographic coordinate r . The cut-off is introduced in order to break the conformal invariance in the IR, and eventually to model color confinement. The location of the cut-off at $r = r_0$, is dual to the dynamically generated energy scale of QCD as $\Lambda_{QCD} \sim 1/r_0$. We shall refer to this solution, as the “AdS cavity” for short.

The model captures many basic features of QCD: one finds a discrete glueball spectrum by studying the fluctuations of the metric, an area law for the Wilson loop by studying classical string embeddings [14], etc. However, the real success of the

model is in the meson sector and indeed the intention of the authors of [8] was to apply it there. In all of the 5D models that are discussed in this paper, the meson sector is generated by space-filling $D4$ and $\overline{D4}$ branes. The fluctuations of the brane fields produce the meson spectra. In addition to reproducing certain generic features such as chiral symmetry breaking, existence of Nambu-Goldstone fields, Gell-Mann-Oaks-Renner relation, one finds %9 agreement with experimental data in the 1^\pm , 0^\pm and 1^{++} spectra.

Yet, the model is crude in many ways, especially when it comes to the glue sector. Running of the gauge coupling is not taken into account; not only the electric but also the magnetic quarks are confined (the 't Hooft loop also exhibits an area law); there is an ambiguity in computation of the glueball masses and related to this there is a degeneracy in the 2^{++} and 0^{++} glueballs [12]; both the glueball and meson spectra are quadratic for large orbital quantum numbers. This list can be largely expanded, but here we shall focus our attention on the thermodynamics of the model and show that the model does not correctly fulfill expectations for the finite temperature physics either.

2.2 Thermodynamics of the Hard-Wall

Some thermodynamical aspects of the hard-wall model is investigated in [10]. At finite temperature there are two competing solutions with the same asymptotics on the boundary: i) a thermal graviton gas which is just the AdS cavity with compact Euclidean time of circumference $1/T$ ii) the AdS black-hole solution with horizon at $r = r_h$. The temperature is related to the location of horizon as $T = 1/\pi r_h$. As one heats up the black-hole, the horizon expands and at a particular temperature it coincides with the IR cut-off $r_h = r_0$. This is the minimum temperature for presence of the black-hole inside the AdS cavity $T_{min} = 1/\pi r_0$. To find out the true minimum of the free energy, one computes the action evaluated on i) and ii) and then one takes the difference, see [10] for details.

Let us define the IR scale as $\Lambda = 1/r_0$. Then, the free energy density¹ for the hard-wall model, for $T > T_{min}$ reads²,

$$f_{HW} = (M_p \ell)^3 \Lambda^4 \left[2 - \pi^4 \left(\frac{T}{\Lambda} \right)^4 \right]. \quad (2.1)$$

Here M_p is the Planck scale and ℓ is the AdS radius. One finds a confinement-deconfinement phase transition at $T_c = 2^{\frac{1}{4}} \Lambda / \pi$. The pressure density is given by $p_{HW} = -f_{HW}$.

¹A word on notation: We shall define the thermodynamic *densities* as the thermodynamic function divided by the volume of the 3D space V_3 times the number of degrees of freedom N_c^2 . For example the entropy density is $s = S/(V_3 N_c^2)$.

²Our notation for the action reads $S = -M_p^3 N_c^2 \int \sqrt{g}(R + V)$. Note that this involves an extra factor of 2 with respect to [10] where his κ is related to our M_p as $\kappa^{-1} = M_p^{\frac{3}{2}} N_c$.

In order to compare the analytic results of the hard-wall model with the lattice data for QCD, one should fix the various energy scales in the model, *i.e.* $M_p\ell$ and Λ . The latter is usually fixed by comparing the vector meson spectrum of the model with the lattice data[8]. One obtains $\Lambda = 323$ MeV. This, in particular yields a transition temperature at $T_c = 122.3$ MeV [10], (see eq. (2.1)).

Fixing the Planck mass is more tricky. The most rigorous way is by comparing the high T asymptotics of QCD and the holographic model. At very high temperatures, the (quenched) QCD becomes a free gas of gluons with a limit value for the pressure density $p_{QCD}/T^4 \rightarrow \pi^2/45$ as $T \rightarrow \infty$. In the hard-wall model, we find from (2.1) that the same quantity limits to $(M_p\ell)^3\pi^4$. Equating the two yields,

$$M_p\ell = (45\pi^2)^{-\frac{1}{3}}. \quad (2.2)$$

We stress that *this is a universal, model independent way of fixing the Planck mass*: One obtains the same value for all of the models discussed in this paper. This is guaranteed to happen quite generally, if the geometry asymptotes to an AdS black-hole near the boundary.

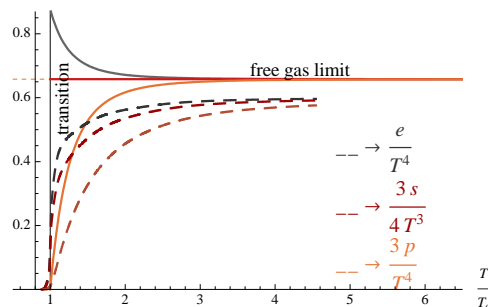


Figure 1: Comparison of the energy, entropy and pressure densities in the HW model with the lattice data of Boyd et al. (dashed curves).

Having fixed all of the parameters in the model, we can compare the thermodynamic functions derived from the HW model with the lattice results. From (2.1) follow all thermodynamic quantities by standard rules. The entropy density can either be found by $s = -df/dT$ or by the Bekenstein-Hawking formula which relates it to the area of the horizon. Eventually, the energy density follows from $e = f + sT$. All in all, one has,

$$s_{HW} = 4(M_p\ell)^3\pi^4T^3, \quad e_{HW} = (M_p\ell)^3\Lambda^4 \left[2 + 3\pi^4 \left(\frac{T}{\Lambda} \right)^4 \right], \quad (2.3)$$

where $M_p\ell$ is given by (2.2). Energy, entropy and pressure are compared in fig. 1. Clearly, there is poor agreement. In particular s/T^3 is constant in the model as a result of the underlying AdS geometry and e/T^4 is a decreasing function unlike in QCD.

The latent heat is defined as the energy density at the phase transition. The lattice value[15] is $L_h = (0.77T_c)^4$. From (2.3) one finds a finite latent heat also in the HW model, $L_h = 8(M_p\ell)^3\Lambda^4 = (0.97T_c)^4$. As this is a finite quantity, *the transition is of first order*.

Presence of a first order deconfinement transition is in accord with our expectations from large N_c QCD [15]. However, there are other shortcomings of the model. First, the conformal anomaly T_μ^μ is a non-trivial function of T in QCD, see fig. 3 whereas this functional dependence is lost in the hard-wall model. One can compute this as $T_\mu^\mu/(V_3N_c^2) = e_{HW} - 3p_{HW}$ from (2.1) and (2.3) and one finds a constant $T_\mu^\mu = 8N_c^2V_3(M_p\ell)^3\Lambda^4$. Similarly, the speed of sound can be computed as $c_s^2 = s/c_v$ where $c_v = de/dT$ is the specific heat of the system, and one finds $c_s^2 = 1/3$. This, of course reflects the fact that the underlying geometry is AdS, and is in complete disagreement with QCD where c_s is again expected to be a non-trivial function of T, see fig. 3.

Secondly, when one computes the bulk viscosity from the Kubo's formula (see [16] for a recent treatment) one finds that $\zeta/s = 0$ which is again in disagreement with QCD. This latter result is rather disappointing because ζ/s is considered to be an important observable probing the quark-gluon plasma at RHIC, and its profile as a function of T reveals important information regarding the nature of the phase transition. In particular, both from the low energy theorems and lattice studies [18], it is expected to make a peak near T_c .

Although there are numerous shortcomings of the the HW model³, it should be viewed as a first step in a holographic approach, instead of a rigorous construction. Indeed, even the fact that such a simple model captures certain basic aspects of QCD is astonishing and should be taken as a starting point for a deeper investigation.

2.3 Soft-wall model

Motivated by the partial success of the HW model in the meson sector, Karch et al. introduced an improvement in [20] that softens the breaking of conformality in the IR. This is achieved by replacing the hard-wall at r_0 by a non-trivial dilaton profile,

$$\phi(r) = (\Lambda r)^2. \tag{2.4}$$

This introduces a dimensionful parameter Λ that sets the scale of the problem in the IR. The geometry is still taken to be AdS_5 .

³The consistency of the model is also questionable. As discussed in [10] and motivated by the critical string-theory constructions such as [19], the IR brane in the AdS cavity is viewed as an “end of space-time” as opposed to a boundary. However, from the point of 5D Einstein gravity, the IR brane really acts as a boundary of the geometry in the deep interior. Thus, in principle one should allow for a Gibbons-Hawking term also at the location of the IR brane. The authors of [17] investigated this issue and found that the deconfinement transition goes away, once a Gibbons-Hawking term is added at the IR brane.

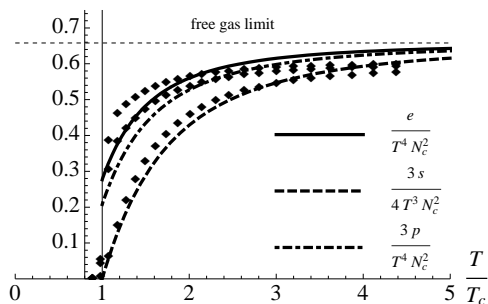


Figure 2: Comparison of the energy, entropy and pressure densities in the SW model with the lattice data of Boyd et al. The diamonds refer to lattice data.

One nice feature of the soft-wall model is linear confinement: The meson spectrum is linear for large orbital excitation number and for large spin, as opposed to the quadratic spectrum of the hard-wall[20]. However, some of the unphysical features in the HW carry over in the glue sector. In particular, there is no running gauge coupling⁴, and magnetic quarks are confined.

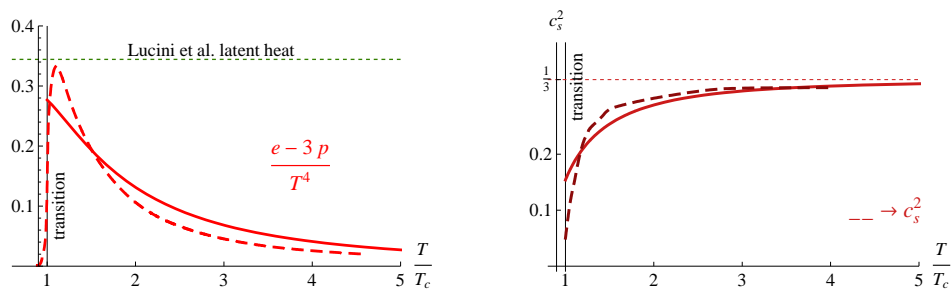


Figure 3: Comparison of the trace anomaly and the speed of light in the SW model with the lattice data of Boyd et al. (dashed curves).

Another main issue is that, the model is non-dynamical, *i.e.* it does not follow from a 5D gravitational action. Instead, the metric and the dilaton profile are imposed by hand⁵. Related to this, computation of the glueball spectra from the bulk-fluctuations is ill defined. Below, we shall see other problematic features at finite T⁶.

⁴One may think of $\Phi(r)$ as a holographic dual to a running coupling, but this identification is problematic for non-dynamical fields.

⁵In [21] a dynamical Einstein-dilaton-tachyon theory is constructed that admits SW as a solution. However it is hard to understand the presence of Tachyon both in the gauge theory and in gravity.

⁶The authors of [20] did not intend to apply the model to the glue sector. As a phenomenological model designed to describe the meson physics in the quenched approximation it is indeed appropriate and the question of whether it solves the equations of motion is not crucial. As we discuss below, it becomes crucial when applied to thermodynamics of glue.

2.4 Thermodynamics of the Soft-Wall

The study of thermodynamics on this background is initiated in [10]. Once again, one considers two competing solutions at finite T : (i) the SW geometry with compact Euclidean time. (ii) AdS black-hole, appended with the non-trivial dilaton profile (2.4). As already mentioned, the construction is non-dynamical, hence neither of these two geometries solve the equations of motion of a 5D Einstein-dilaton system. One assumes that they are solutions to some unspecified gravitational theory and computes the free energy density with the prescription described in section 2.2 [10]. The result is,

$$f_{SW} = 2(M_p \ell)^3 T^4 \left[\frac{1}{2} + e^{-\left(\frac{\Lambda}{\pi T}\right)^2} \left(\left(\frac{\Lambda}{\pi T} \right)^2 - 1 \right) 2 + \left(\frac{\Lambda}{\pi T} \right)^4 Ei\left[-\left(\frac{\Lambda}{\pi T} \right)^2\right] \right]. \quad (2.5)$$

Here Λ is the parameter that appears in (2.4) and Ei is the exponential-integral function. One obtains a phase transition at $T_c = 0.4917\Lambda$. As before, one can fix the value of Λ by matching the lowest ρ meson mass and one finds, $\Lambda = 338$ MeV which yields a T_c better than HW, $T_c = 191$ MeV [22]. The latent heat also turns out better than the HW model. One finds $L_h = (0.725T_c)^4$ that is very close to the Lucini et al.'s lattice result of $(0.77T_c)$.

The non-dynamical feature of the model manifests itself in the computation of entropy. The entropy as computed from the Bekenstein-Hawking formula and from $s = -df/dT$ above do not match. The BH geometry does not obey the laws of thermodynamics, which makes the findings questionable. However, let us press on, and assume that one indeed obtains a free energy of the form (2.5) from some unspecified dynamical theory and work out other thermodynamic functions. The computation is just as in the HW case and the results are summarized in figs. 2 and 3. These results are in very good agreement with the lattice study of [23].

It is surprising that a non-dynamical theory, constructed with many assumptions yield such good results and it begs for a better understanding. We shall, in the next section, investigate a *dynamical* dilaton-Einstein system with solutions similar to the form (2.4) in the large r region.

An underlying dynamical theory is needed also to compute certain important observables such as the bulk viscosity ζ . In the holographic set-up, this quantity is computed using Kubo's formula [16]. The reason this computation is ill-defined in the SW model is that one needs to solve for the bulk fluctuations in an holographic computation and this requires that the background solves Einstein's eqs.

3. Non-critical holographic QCD

3.1 Dynamical Models

There is a long history of the dilaton-gravity systems in the context of the AdS/CFT

correspondence. Due to lack of space, we are not able to provide an exhaustive list of references here. Rather we shall mention a few articles that are closely related to our approach. The papers [24] demonstrated that type 0 string theory provides a fruitful set-up for gravity duals of running gauge coupling. They considered a 10D background that involves a dilaton and a bulk tachyon field. Asymptotics of the dilaton in the deep interior exhibits a log-running of the gauge coupling! (however, presence of the tachyon is confusing as there are no obvious dual gauge invariant in the gauge theory). Similarly, Gubser [25] analyzed a dilaton flow in the context of type IIB, truncated to 5D⁷. Other notable papers that study a dynamical dilaton flow in the 5D set-up are [27], [21], [17] and [28]. The latter uses an approach very similar to ours⁸. Finally, Gubser and collaborators [29, 30] recently analyzed the dilaton-gravity system at finite temperature, obtaining results that are quite similar to [13].

3.2 Improved holographic QCD

There are many reasons supporting a non-fermionic (such as type 0 string theories) and a non-critical holographic approach[31]. From an economic point of view, five dimensions provide all the necessary degrees of freedom to construct a dual of QCD: four dimensions where the gauge theory lives, plus a radial direction dual to the energy scale of the gauge theory. Furthermore, a brief study of the low energy degrees of freedom of 5D non-critical string theory yields a nice correspondence between the various objects in string theory and gauge theory [11]. Absence of extra dimensions, hence absence of the undesired Kaluza-Klein degrees of freedom is another attractive feature.

The only non-trivial bulk fields required to model the low energy dynamics of large N_c QCD are the metric (dual to the energy-momentum tensor), the dilaton (dual to λ_{YM} and $\text{Tr}F^2$) and the axion⁹ (dual to θ_{YM} and $\text{Tr}F \wedge F$). Here, we shall present such a set-up [11, 12] and describe its zero temperature solutions. A simple 5D action is,

$$S_5 = -M_P^3 N_c^2 \int d^5x \sqrt{g} \left[R - \frac{4}{3}(\partial\Phi)^2 + V(\Phi) \right] + 2M_P^3 N_c^2 \int_{\partial M} d^4x \sqrt{h} K. \quad (3.1)$$

where V is a yet undetermined potential for the dilaton. The second term above is the Gibbons-Hawking term, K being the extrinsic curvature on the boundary¹⁰.

⁷An early work on dilaton flow in the IIB set-up is [26]

⁸See however below eq. (3.7) for various differences.

⁹We will not be concerned with the axion in this paper. Its action is suppressed in the large N_c limit, hence can be consistently ignored. Note however, that the axion sector has very interesting implications for the strong CP violation problem [12].

¹⁰As a boundary term, it has no contribution to the equations of motion and will play no role in this subsection. However, its contribution is crucial in comparing on-shell actions as we discuss in the next subsection.

We make the domain-wall ansatz in order to preserve the 4D Lorentz symmetry. In the conformal coordinate system,

$$ds^2 = e^{2A_0(r)} (dr^2 + \eta_{ij} dx^i dx^j), \quad \Phi = \Phi_0(r). \quad (3.2)$$

Here, $r \geq 0$ is the radial coordinate. Boundary is located at $r = 0$.

The only non-trivial input in (3.1) is the dilaton potential V . In order to fix V we employ requirements from the dual gauge theory. Holographic dictionary relates the scale factor A and the dilaton Φ to the energy scale and the 't Hooft coupling respectively ¹¹:

$$E = e^A, \quad \lambda_{YM} = \lambda \equiv e^\Phi. \quad (3.3)$$

Given these identifications, one can relate the β -function of the gauge theory to V in a one to one fashion[11]. Although the shape of $V(\lambda)$ is not fixed without knowledge of the exact gauge theory β -function, its UV (small λ) and IR (large λ) asymptotics can be determined.

UV asymptotics

In the UV, the input comes from perturbative QCD. We demand asymptotic freedom with logarithmic running. This implies in particular that the asymptotic UV geometry is that of AdS_5 with logarithmic corrections. This requires a (weak-coupling) expansion of $V(\lambda)$ of the form $V(\lambda) = 12/\ell^2(1 + v_1\lambda + v_2\lambda^2 + \dots)$. Here ℓ is the AdS radius and v_i are dimensionless parameters of the potential directly related to the perturbative β -function coefficients of QCD [11]. In conformal coordinates, close to the AdS_5 boundary at $r = 0$, the metric and dilaton behave as ¹²:

$$ds_0^2 = \frac{\ell^2}{r^2} \left(1 + \frac{8}{9} \frac{1}{\log r \Lambda} + \dots \right) (dr^2 + dx_4^2), \quad \lambda_0 = -\frac{1}{\log r \Lambda} + \dots \quad (3.4)$$

where the ellipsis represent higher order corrections that arise from second and higher-order terms in the β -function. The mass scale Λ is an initial condition for the dilaton equation and corresponds to Λ_{QCD} just like in the soft-wall model above.

IR asymptotics

For any asymptotically AdS space, Einstein's equations dictate the geometry in the deep interior be, either another AdS or a singular geometry that terminates at $r = r_0$ [12]. For QCD, it is the second option that is more plausible, as the gauge theory is not conformal invariant in the IR. Details of the IR geometry (or

¹¹In the latter equation, there is an undetermined proportionality constant κ . However it can be set to 1 by a rescaling in the potential and all physical observables turn out independent of this rescaling. Thus, with no loss of generality we can choose $\lambda_{YM} = e^\Phi$.

¹²We will use a "zero" subscript to indicate quantities evaluated at zero temperature.

equivalently the large λ asymptotics of V) are determined by the requirement of color confinement a la [14]. In particular, we require that the quark-antiquark potential is linear. This happens when

$$V(\lambda) \rightarrow \lambda^Q \log^P(\lambda), \quad \lambda \rightarrow \infty, \quad (3.5)$$

and when the parameters Q and P fall into either of the two cases:

$$(i) \quad Q > 4/3, P \text{ arbitrary} \rightarrow r_0 = \text{finite} \quad (3.6)$$

$$(ii) \quad Q = 4/3, P \geq 0 \rightarrow r_0 = \infty. \quad (3.7)$$

In the first case, the geometry terminates at finite r , hence this is somewhat similar to the hard-wall geometry. The latter case similar to the soft-wall geometry as it involves a singularity at $r = \infty$. The asymptotics above also guarantee that the classical string configurations do not reach the singularity at r_0 . The same requirement for the particle-like bulk excitations yield an additional condition in case (i): $Q < 4\sqrt{2}/3$. For $Q \geq 4\sqrt{2}/3$, the glueball spectrum becomes ill-defined[12]. We note that both the geometry in [28] and in [29] fall into this problematic class. These problematic geometries also have undesired features at finite T.

It is shown in [12] that in both cases, the magnetic quarks are screened and the glueball spectrum is gapped and discrete. In case (i) the glueball spectrum turns out to be quadratic whereas in case (ii) the spectrum grows as $w_n \propto n^{2P}$. For phenomenological reasons, the preferred geometry thus corresponds to the linear spectrum with $P = 1/2$. In this case the asymptotic geometry is,

$$ds_0^2 \rightarrow e^{-C(\frac{r}{\ell})^2} (dr^2 + dx_4^2), \quad \lambda_0 \rightarrow e^{3C/2(\frac{r}{\ell})^2} \left(\frac{r}{\ell}\right)^{\frac{3}{4}} \quad (3.8)$$

where the constant C is a positive constant related to Λ in (3.4).

Parameters of the model

The dimensionless parameters of the holographic model a priori are (in AdS length units): the Planck mass $M_p \ell$, which governs the scale of interactions between the glueballs in the theory, the scale $\Lambda \ell$ that plays the role of Λ_{QCD} , the string length scale ℓ_s/ℓ and the parameters v_i that specify the shape of the potential V . The Planck mass is fixed by studying large T asymptotics, exactly as in eq. (2.2). On the other hand, symmetries of the equations guarantee that no physical observable depend on $\Lambda \ell$. The number ℓ/ℓ_s can be determined by comparison with the string tension in lattice QCD. For the particular model that is investigated here, this turns out to be $\ell/\ell_s \approx 8$. This is an encouraging result which shows the α' corrections are suppressed by about order 10.

Finally, we fix the shape of the potential by arbitrarily picking up a function V that satisfies the UV and the IR asymptotics discussed above. A function that does the job is,

$$V(\lambda) = \frac{12}{\ell^2} \left(1 + v_1 \lambda + v_2 \lambda^{\frac{4}{3}} \log^{\frac{1}{2}} \left(1 + v_3 \lambda^{\frac{4}{3}} + v_4 \lambda^2 \right) \right). \quad (3.9)$$

We shall specify the numbers v_i in the following.

The units in the problem can be fixed by matching the lowest lying 0^{++} glueball in our model and in lattice QCD¹³ [12]. This also fixes the the actual value of the Planck scale, $M_p N_c^{2/3}$. If one wants to compare results of the model with a gauge theory with finite N_c , this value gives a cut-off, above which one cannot ignore string interactions. For $N_c = 3$ one has $M_p N_c^{2/3} \approx 2.5$ GeV. Of course there is no such a cut-off in large N_c QCD.

4. Thermodynamics of Improved Holographic QCD

Having defined the theory at zero T, now we look for finite T solutions. At finite temperature there exist two distinct types of solutions to the action (3.1) with AdS asymptotics, (3.4):

- i. The thermal graviton gas, obtained by compactifying the Euclidean time in the zero temperature solution with $\tau \sim \tau + 1/T$:

$$ds^2 = e^{2A_0(r)} (dr^2 + d\tau^2 + dx_3^2), \quad \lambda = \lambda_0(r). \quad (4.1)$$

This solution exists for all $T \geq 0$ and corresponds to a confined phase, if the gauge theory at zero T confines.

- ii. The black hole (BH) solutions (in Euclidean time) of the form:

$$ds^2 = e^{2A(r)} \left(\frac{dr^2}{f(r)} + f(r) d\tau^2 + dx_3^2 \right), \quad \lambda = \lambda(r). \quad (4.2)$$

The function $f(r)$ approaches unity close to the boundary at $r = 0$. There exists a singularity in the interior at $r = \infty$ that is now hidden by a regular horizon at $r = r_h$ where f vanishes. Such solutions correspond to a deconfined phase.

As we discuss below, in confining theories the BH solutions exist only above a certain minimum temperature, $T > T_{min}$.

The thermal gas solution has only two parameters: T and Λ . The black hole solution should also have a similar set of parameters: the equations of motion are second order for λ and f , and first order for A [32]. Thus, *a priori* there are 5

¹³According to [35] this is $m_{0^{++}} = 1475$ MeV

integration constants to be specified. A combination of two integration constants of A and λ determines Λ . (The other combination can be removed by reparametrization invariance in r). The condition $f \rightarrow 1$ on the boundary removes one integration constant and demanding regularity at the horizon, $r = r_h$, in the form $f \rightarrow f_h(r_h - r)$, removes another. The remaining integration constant can be taken as f_h (or r_h , they are not independent), related to the temperature by

$$4\pi T = f_h. \quad (4.3)$$

In the large N_c limit, the saddle point of the action is dominated by one of the two types of solutions. In order to determine the one with minimum free energy, we need to compare the actions evaluated on solutions i. and ii. with equal temperature.

We introduce a cutoff boundary at $r = \epsilon$ in order to regulate the infinite volume. The difference of the two scale factors is given near the boundary as [32]:

$$A(\epsilon) - A_0(\epsilon) = \mathcal{G}(T)(\epsilon\Lambda)^4 + \dots \quad (4.4)$$

Then the free energy density is given by [13]:

$$f_{NC} = -p_{NC} = 15(M_p\ell)^3\Lambda^4\mathcal{G}(T) - \frac{T s_{NC}}{4}. \quad (4.5)$$

Here, the entropy density s_{NC} is given by the area of the horizon:

$$s_{NC} = 4\pi^2 M_p^3 e^{3A(r_h)}. \quad (4.6)$$

One can check (by numerics) that this entropy is precisely the same as follows from the 1st law $s = -df/dT$. This is what one expects as the theory defined by (3.1) satisfies the gravitational energy theorems and T is defined in (4.3) by requiring absence of conical singularity at the horizon.

It is clear from (4.5) that presence of the first term is crucial for existence of a phase transition, as the second term by itself is negative definite. Below, we explain the physical meaning of the quantity \mathcal{G} .

Role of the gluon condensate

The quantity \mathcal{G} can also be defined from the difference of the dilatons ($\lambda = \exp(\Phi)$),

$$\Phi(\epsilon) - \Phi_0(\epsilon) = \frac{45}{8}\mathcal{G}(T)(\epsilon\Lambda)^4 \log(\epsilon\Lambda) + \dots \quad (4.7)$$

Now, the meaning of \mathcal{G} becomes clear. The AdS/CFT prescription relates bulk fluctuations with VEVs of dual operators in the gauge theory. As the dilaton couples to the operator $\text{Tr}F^2$, we learn that \mathcal{G} is the difference of VEVs in the gluon condensate at finite and zero temperatures: $\mathcal{C}(T) \propto \langle \text{Tr}F^2 \rangle_T - \langle \text{Tr}F^2 \rangle_0$.

Let us perform a consistency check. The dilatation Ward identity in gauge theory relates the condensate to the energy-momentum tensor: $\langle T_\mu^\mu \rangle_{T0} = -\frac{\beta}{4\lambda^2} \langle \text{Tr} F^2 \rangle_{T0}$. The subscript refers to the difference finite and zero T. We shall check this identity in the holographic set-up (at leading order in λ). The LHS follows from $T_\mu^\mu = \epsilon_{NC} - 3p_{NC}$. The energy e_{NC} is derived from (3.1), one finds

$$T_\mu^\mu = 60(M_p \ell)^3 \Lambda^4 \mathcal{G}. \quad (4.8)$$

The RHS of the Ward identity is computed by the AdS/CFT prescription: For any canonically normalized bulk fluctuation for $\chi(x) = r^{\Delta_-} \chi_0(x) + r^{\Delta_+} \chi_1(x)$ near the boundary, the VeV of the dual operator is $\langle \mathcal{O}(x) \rangle = (2\Delta_+ - d)\chi_1(x)$. Taking χ as $\delta\Phi$ in (4.7)¹⁴, we find $\langle \text{Tr} F^2 \rangle_{T0} = \frac{240(M_p \ell)^3 N_c^2 \Lambda^4}{b_0} \mathcal{G}$. Using the β -function $\beta(\lambda) = -b_0 \lambda^2 - \dots$ we see that this precisely matches the RHS of the Ward identity given by (4.8).

One may wonder why it works. After all, the prescription is conjectured for the pure AdS space and we have a log-corrected AdS here. The reason is that, one can generalize the holographic renormalization program of AdS to this geometry by explicitly computing the counter-terms [33] and show that the contribution from the counter-terms cancel out precisely between the finite and zero T components.

Existence and order of the deconfinement transition

For a general potential V that obeys the UV and IR asymptotics described in the previous subsection, we can prove the following statements:

- i. *There exists a phase transition at finite T , if and only if the zero- T theory confines as in (3.6) or (3.7)*
- ii. *This transition is of the **first order** for all of the confining geometries, with a single exception described in iii:*
- iii. *In the limit confining geometry $P = 0$ of (3.7), $A_0(r) \rightarrow -Cr$ (as $r \rightarrow \infty$), the phase transition is of the **second order** and happens at $T = 3C/4\pi$.*
- iv. *All of the non-confining geometries at zero T are always in the black hole phase at finite T . They exhibit a second order phase transition at $T = 0^+$.*

An heuristic demonstration is given in [13] and a general, coordinate independent proof will appear in [32]. Here, let us only mention that the crucial element for the phase transition in confining geometries is the existence of (i) a “big” black-hole with positive specific heat for small r_h and (ii) a “small” black-hole with negative specific

¹⁴One should be careful about the multiplicative factors arising from normalization of Φ in (3.1), see [32].

heat for large r_h . Co-existence of big and small black-holes is just as in AdS BHs *with spherical horizon*. See fig. 4 for an illustration. It is clear from this figure that there exists a T_{min} for the confining geometries as in eq. (3.7), below which both BHs disappear.

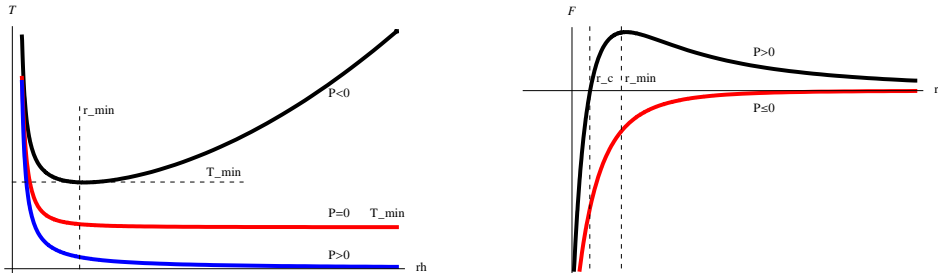


Figure 4: Schematic behavior of temperature and free energy as functions of r_h , for the infinite- r geometries of the type (3.7), for different values of P .

Numerical Results

The numerical results that we review in this section are based on [34]. All the thermodynamic properties of the system follow from (4.5). One numerically solves the Einstein-dilaton system for a fixed Λ ¹⁵ and for different r_h , corresponding to different T (see fig. 4) to obtain $s_{NC}(T)$ and $\mathcal{G}(T)$. The rest follows from the laws of thermodynamics. The potential is chosen in (3.9). Only three of the v_i are independent because, as mentioned earlier, the physics is left invariant under the rescaling $\lambda \rightarrow \kappa\lambda$. We fix one combination of v_i to match the lattice result for the latent heat $L_h = (0.75T_c)^4$. The two other parameters are chosen in order to obtain good glueball mass ratios¹⁶. A good set of parameters is $\{v_1, v_2, v_3, v_4\} = \{0.1, 46, 0.05, 1000\}$.¹⁷ The rest of the results in this section are predictions.

We find a transition temperature at $T_c \approx 247$ MeV which is very close to lattice [15].¹⁸ The thermodynamic functions ϵ_{nc} , s_{nc} and p_{nc} are compared with the lattice data in fig. 5, left. The temperature dependence of the gluon condensate is shown and compared to lattice in fig. 5, right. The speed of sound and the bulk viscosity are presented in fig. 6.¹⁹ We conclude that the model presented here is in very good agreement with the available lattice data.

¹⁵This is the same in both geometries and fixed by the lowest 0^{++} mass as $\Lambda \approx 290$ MeV.

¹⁶We shall not discuss the glueball spectrum here, see [34]. With the potential above, one obtains e.g. $m_{0^{++*}}/m_{0^{++}} = 1.6$ which is in well agreement with lattice [35].

¹⁷The difference in these coefficients and the ones in [34] are due to a different choice of κ here.

¹⁸This value is for $SU(N_c)$ YM in the large N_c limit which is significantly different from both the QCD value and the SW model cited in sec. 2.4.

¹⁹The derivation of numerical results on the bulk viscosity, along with other dynamical observables will appear in [36].

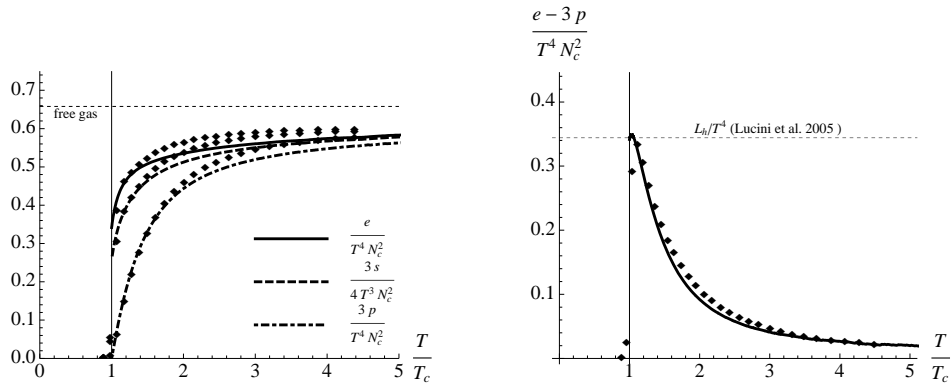


Figure 5: Dimensionless thermodynamic functions and the gluon condensate. The diamonds correspond to the lattice data of Boyd et al.

A last word on the bulk viscosity. Both the low-energy theorems and the lattice arguments [18] indicate that the bulk viscosity has a peak near T_c . This is what we also observe in fig. 6, however the height of the peak is less than the lattice evaluation [37]²⁰, see also [16] for the same conclusion.

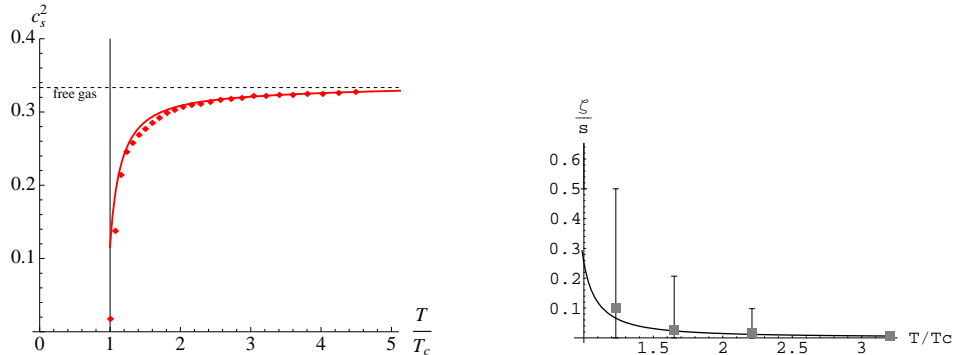


Figure 6: Left: Comparison of speed of sound in our model and the lattice result of Boyd et al. (diamonds). Right: Comparison of the bulk viscosity with the lattice data of Meyer.

5. Discussion and Outlook

We presented a holographic model for large N_c QCD at finite T , that resolves most of the problematic issues of the AdS/QCD models and yields very good agreement with the available lattice data. The deconfinement transition results from presence of a non-trivial gluon condensate. We also demonstrated that the AdS/CFT prescription for computing n-point functions carry over if computed as differences at finite and

²⁰Note however that computation of this quantity on the lattice is notoriously difficult and afflicted with numerical errors that arise from analytic continuation.

zero T . Strictly speaking, the model is valid at large N_c . For finite N_c , there exists a UV cut-off, which is about 2.5 GeV for $N_c = 3$. The α' corrections are somewhat under control as the AdS radius is order 10 in string units. However, generally one expects corrections from the higher string modes.

One related problem of all two-derivative effective actions is that the shear viscosity - entropy ratio is universally fixed as $\eta/s = 1/4\pi$ [38], rather than a function of T as expected in QCD. In order to cure this problem, one should consider higher derivative corrections in the action. Other possible future directions include study of the meson sector via probe D4 branes, turning on a baryon chemical potential by charged BHs and eventually searching for explicit non-critical or critical string theory backgrounds where the solutions can be embedded.

Acknowledgments

Some of the results on the thermodynamics of the HW and SW models, and all of the results in sec. 3 were derived in collaboration with E. Kiritsis, L. Mazzanti and F. Nitti. We thank E. Kiritsis and K. Peeters for a careful reading and comments. This work was supported by the VIDI grant 016.069.313 from the Dutch organization for Scientific Research (NWO).

References

- [1] K. Adcox *et al.* [PHENIX Collaboration], Nucl. Phys. A **757** (2005) 184 [arXiv:nucl-ex/0410003].
- [2] J. M. Maldacena, Adv. Theor. Math. Phys. **2**, 231 (1998) [Int. J. Theor. Phys. **38**, 1113 (1999)]
- [3] G. Policastro, D. T. Son and A. O. Starinets, Phys. Rev. Lett. **87** (2001) 081601 [arXiv:hep-th/0104066].
- [4] H. Liu, K. Rajagopal and U. A. Wiedemann, Phys. Rev. Lett. **97** (2006) 182301 [arXiv:hep-ph/0605178].
- [5] S. S. Gubser, Phys. Rev. D **74** (2006) 126005 [arXiv:hep-th/0605182].
- [6] T. Sakai and S. Sugimoto, Prog. Theor. Phys. **113** (2005) 843 [ArXiv:hep-th/0412141].
- [7] J. Polchinski and M. J. Strassler, Phys. Rev. Lett. **88** (2002) 031601 [ArXiv:hep-th/0109174];
- [8] J. Erlich, E. Katz, D. T. Son and M. A. Stephanov, Phys. Rev. Lett. **95**, 261602 (2005) [arXiv:hep-ph/0501128]; L. Da Rold and A. Pomarol, Nucl. Phys. B **721**, 79 (2005) [ArXiv:hep-ph/0501218].

- [9] E. Witten, Adv. Theor. Math. Phys. **2** (1998) 505 [ArXiv:hep-th/9803131].
- [10] C. P. Herzog, Phys. Rev. Lett. **98**, 091601 (2007) [ArXiv:hep-th/0608151].
- [11] U. Gursoy and E. Kiritsis, JHEP **0802** (2008) 032 [ArXiv:0707.1324] [hep-th].
- [12] U. Gursoy, E. Kiritsis and F. Nitti, JHEP **0802** (2008) 019 [ArXiv:0707.1349] [hep-th].
- [13] U. Gursoy, E. Kiritsis, L. Mazzanti and F. Nitti, Phys. Rev. Lett. **101** (2008) 181601 [arXiv:0804.0899] [hep-th].
- [14] S. J. Rey and J. T. Yee, Eur. Phys. J. C **22** (2001) 379 [arXiv:hep-th/9803001]; J. M. Maldacena, Phys. Rev. Lett. **80** (1998) 4859 [arXiv:hep-th/9803002].
- [15] B. Lucini, M. Teper and U. Wenger, JHEP **0502** (2005) 033 [arXiv:hep-lat/0502003].
- [16] S. S. Gubser, S. S. Pufu and F. D. Rocha, JHEP **0808** (2008) 085 [arXiv:0806.0407] [hep-th].
- [17] N. Evans and E. Threlfall, arXiv:0805.0956 [hep-th].
- [18] D. Kharzeev and K. Tuchin, JHEP **0809** (2008) 093 [arXiv:0705.4280] [hep-ph]; F. Karsch, D. Kharzeev and K. Tuchin, Phys. Lett. B **663** (2008) 217 [arXiv:0711.0914] [hep-ph].
- [19] I. R. Klebanov and M. J. Strassler, JHEP **0008** (2000) 052 [ArXiv:hep-th/0007191].
- [20] A. Karch, E. Katz, D. T. Son and M. A. Stephanov, “*Linear confinement and AdS/QCD*,” Phys. Rev. D **74** (2006) 015005 [ArXiv:hep-ph/0602229].
- [21] B. Batell and T. Gherghetta, Phys. Rev. D **78** (2008) 026002 [arXiv:0801.4383] [hep-ph].
- [22] F. Karsch, J. Phys. Conf. Ser. **46** (2006) 122 [arXiv:hep-lat/0608003].
- [23] G. Boyd, J. Engels, F. Karsch, E. Laermann, C. Legeland, M. Lutgemeier and B. Petersson, “*Thermodynamics of SU(3) Lattice Gauge Theory*,” Nucl. Phys. B **469**, 419 (1996) [ArXiv:hep-lat/9602007].
- [24] I. R. Klebanov and A. A. Tseytlin, Nucl. Phys. B **547** (1999) 143 [arXiv:hep-th/9812089]; J. A. Minahan, JHEP **9901** (1999) 020 [arXiv:hep-th/9811156].
- [25] S. S. Gubser, arXiv:hep-th/9902155.
- [26] A. Kehagias and K. Sfetsos, Phys. Lett. B **454** (1999) 270 [arXiv:hep-th/9902125];
- [27] S. Nojiri and S. D. Odintsov, Phys. Lett. B **458** (1999) 226 [arXiv:hep-th/9904036].
- [28] C. Csaki and M. Reece, JHEP **0705** (2007) 062 [ArXiv:hep-ph/0608266].
- [29] S. S. Gubser, A. Nellore, S. S. Pufu and F. D. Rocha, Phys. Rev. Lett. **101** (2008) 131601 [arXiv:0804.1950] [hep-th].

- [30] S. S. Gubser and A. Nellore, arXiv:0804.0434 [hep-th].
- [31] A. M. Polyakov, Int. J. Mod. Phys. A **14** (1999) 645 [arXiv:hep-th/9809057].
- [32] U. Gursoy, E. Kiritsis, L. Mazzanti and F. Nitti, arXiv:0812.0792 [hep-th].
- [33] U. Gursoy, I. Papadimitriou, to appear.
- [34] U. Gursoy, E. Kiritsis, L. Mazzanti and F. Nitti, arXiv:0903.2859 [hep-th].
- [35] H. B. Meyer, arXiv:hep-lat/0508002.
- [36] U. Gursoy, E. Kiritsis, G. Michalogiorgakis and F. Nitti, to appear.
- [37] H. B. Meyer, Phys. Rev. Lett. **100** (2008) 162001 [arXiv:0710.3717 [hep-lat]].
- [38] A. Buchel and J. T. Liu, Phys. Rev. Lett. **93** (2004) 090602 [arXiv:hep-th/0311175].